

Notes

Prediction of the Linear Viscoelastic Shear Modulus of an Entangled Polybutadiene Melt from Simulation and Theory

Oleksiy Bytner and Grant D. Smith*

Department of Chemical and Fuels Engineering and
Department of Materials Science and Engineering,
122 S. Central Campus Drive Rm. 304, University of Utah,
Salt Lake City, Utah 84112

Received March 10, 2000

Revised Manuscript Received October 16, 2000

I. Introduction

While accurate quantum chemistry based potentials,¹ improved simulation algorithms, and faster computers have made accurate calculation of chain dynamics in unentangled polymer melts from molecular dynamics simulations possible,^{2–5} direct calculation of the viscoelastic properties of entangled polymers remains well beyond the capability of even the most powerful computers. Encouragingly, polymer melt dynamics of chains below the entanglement length can be represented reasonably well by the Rouse model^{6,7} while the molecular theory of viscoelasticity of Doi and Edwards^{7–11} based on the reptating chain model of de Gennes¹² has proven successful in describing entangled melts. Until now, the structural, thermodynamic, and dynamic properties required by these models have been obtained exclusively from experiment. In this paper we utilize the results of molecular dynamics (MD) simulations of an unentangled polybutadiene (PBD) melt in the prediction of the linear viscoelastic response of an entangled melt and compare the calculated complex shear modulus with experiment.

II. Molecular Dynamics Simulations

We performed MD simulations of a PBD melt using the quantum chemistry based potential described elsewhere.^{5,13} An ensemble of 40 random copolymer chains each comprised of 30 units with a microstructure of 40%/50%/10% 1,4-cis/1,4-trans/1,2-vinyl monomers was generated.⁵ Each chain consisted of 114 backbone carbons (BD₁₁₄), which is slightly below the entanglement molecular weight for this polymer.¹⁴ After equilibration, constant temperature and density sampling trajectories of 30, 60, and 130 ns were generated at 353, 323, and 293 K, respectively. An extensive comparison at 353 K with NMR spin–lattice and neutron spin-echo measurements performed on the same molecular weight material revealed that the MD simulations using the quantum chemistry force field accurately reproduce the local and chain dynamics of the unentangled PBD chains.^{5,15}

III. Reptation Models

To obtain the time-dependent shear stress modulus $G(t)$ and frequency-dependent complex shear modulus

$G^*(\omega)$ for entangled melts, specifically BD₉₁₄₀ (130 000 Da) for which experimental data exist, we have employed three reptation models: (i) the original reptation model of Doi and Edwards^{7–10} (DE); (ii) a modified version of DE that accounts for fluctuations of the chain contour length¹¹ (MDE); (iii) an additional reptation model that accounts for contour-length fluctuations presented by Milner and McLeish.¹⁶ The principal relationships used in these models as well as crossover functions between dynamic regimes are outlined in Tables 1 and 2. These models require only a few parameters for calculation of $G(t)$ and $G^*(\omega)$, specifically the Rouse time τ_R , the number of bonds between entanglements N_e , the plateau modulus G_N , and a glassy modulus G_∞ , all of which can be obtained directly or indirectly from simulations of unentangled melts, as demonstrated below.

Rouse Time and the Monomer Friction Coefficient. The fundamental relaxation time in the reptation model is the Rouse time τ_R given by⁷

$$\tau_R = \frac{\zeta N \langle R^2 \rangle}{3\pi^2 k_B T} \quad (1)$$

where ζ is the monomer friction coefficient, N is the number of backbone bonds in the chain, $\langle R^2 \rangle$ is the mean-square end-to-end distance, and T is the absolute temperature. The monomer friction coefficient is the only dynamic parameter in both the Rouse and reptation models; it expresses the effective medium viscous force acting on a monomer per unit velocity.

Graessley¹⁷ found that ζ can be determined from the measured viscosity of low molecular weight polymers, yielding reasonable agreement with experiment for the diffusion coefficient of high molecular weight polymers. These results indicate that ζ is not strongly dependent upon the polymer chain length. Hence, we neglected any molecular weight dependence of ζ . For unentangled chains, the Rouse model yields the monomer friction coefficient as⁷

$$\zeta(T) = \frac{3\pi^2 k_B T \tau_R}{N \langle R^2 \rangle} = \frac{k_B T}{D(T)N} \quad (2)$$

where $D(T)$ is the temperature-dependent self-diffusion coefficient determined from the mean-square center-of-mass displacement of the unentangled polymer chains. For BD₁₁₄, τ_R and $D(T)$ were found to be in excellent agreement with experiment⁵ and yielded consistent values for the monomer friction coefficient. The Rouse time for a polymer of any molecular weight (entangled or not) can be determined from the relationship⁷

$$\tau_R = \tau_R^0 \left(\frac{N}{N_0} \right)^2 \quad (3)$$

Table 1. Time-Dependent Shear Stress Moduli in Different Regimes for Different Reptation Models^a

$G(t) = G_{glass}(t) + G_A(t) + G_{Rouse}(t) + G_{rept}(t)$			
Function	DE ^b	MDE ^c	Milner-McLeish ^d
Glassy regime $G_{glass}^{e,f}$	$G_\infty (1 - erf(\sqrt{t/\tau_0}))$	$G_\infty (1 - erf(\sqrt{t/\tau_0}))$	$G_\infty (1 - erf(\sqrt{t/\tau_0}))$
Retraction regime G_A	-	$\frac{4}{5} G_N \sum_{p=1}^{N_e} \exp\left(-\frac{2tp^2}{\tau_A}\right)$	$G_N \int_0^{s_d} 2(1-s) \exp\left(-\frac{t}{\tau(s)}\right) ds$
Rouse regime G_{Rouse}	$\frac{G_N}{n} \sum_{p=1}^{\infty} \exp\left(-\frac{2tp^2}{\tau_R}\right)$	$\frac{G_N}{n} \sum_{p=1}^n \exp\left(-\frac{tp^2}{\tau_R}\right)$	$\frac{G_N}{n} \sum_{p=1}^N A(p) \exp\left(-\frac{tp^2}{\tau_R}\right)^g$
Reptating regime G_{rept}	$G_N \sum_{p, odd}^{\infty} \frac{8}{\pi^2 p^2} \exp\left(-\frac{tp^2}{\tau_d}\right)$	$G_N \int_0^1 \exp\left(-\frac{t}{\tau(s)}\right) ds$	$G_N \sum_{p, odd}^{\infty} \frac{8}{\pi^2 p^2} \exp\left(-\frac{tp^2}{\tau_d}\right)$
Crossover functions	-	$\tau(s) = \tau_A \begin{cases} \frac{3}{16} n^4 s^4; & s < 2n^{-1/2} \\ 3(s - n^{-1/2})^2 n^3; & s \geq 2n^{-1/2} \end{cases}$	$\tau(s) = \tau_A \frac{225}{256} \pi^3 n^4 s^4$
	-	-	$s_d = \frac{\sqrt{1 + 4\left(\frac{225}{256} \pi^3 n\right)^{1/2}} - 1}{2\left(\frac{225}{256} \pi^3 n\right)^{1/2}}$
Longest relaxation time	$\tau_d = 3n^3 \tau_A$	$\tau_d = 3n^3 (1 - n^{-1/2})^2 \tau_A$	$\tau_d = 3n^3 (1 - s_d)^2 \tau_A$

^a N , N_e , and n are the same as in eq 6; $\tau_A = n^{-2}\tau_R$ and τ_R is given by eq 1; G_N and G_∞ are given by eqs 9 and 14, respectively. ^b References 7–10. ^c References 11 and 21. ^d Reference 16. ^e The same for all three models, refs 21 and 24. ^f τ_0 is given by eq 12. ^g $A(p) = 1$, if $p \leq n$, and $A(p) = 1/3$, if $p > n$.

where τ_R^0 and N_0 are the Rouse time and number of backbone bonds for the unentangled reference system.

Plateau Modulus and the Number of Bonds between Entanglements. The value of the plateau modulus G_N for entangled polymeric systems is given as⁷

$$G_N = \frac{\rho k_B T}{M_e} = \frac{\rho k_B T}{M_0 N_e} \quad (4)$$

where M_e is molecular weight between entanglements, $M_0 = M/N$ is the molecular weight per backbone bond, and ρ is the melt density. In the reptation model, topological constraints due to entanglements with neighboring chains are considered to form a tube of diameter a enclosing each chain. The quantity a^2 also represents the mean-square distance between neighboring entanglements along the chain. Hence, the number of entanglements n of a chain of N monomers can be written as^{7,14}

$$n = \frac{\langle R^2 \rangle}{a^2} \quad (5)$$

and number of monomers between entanglements N_e as

$$N_e = N \frac{a^2}{\langle R^2 \rangle} \quad (6)$$

The tube diameter cannot be extracted directly from simulations of unentangled chains, but simple scaling arguments indicate that it should be proportional to the packing length P defined as¹⁴

$$P = \frac{M}{\rho \langle R^2 \rangle} \quad (7)$$

where M is the polymer molecular weight. It has been shown empirically for a large variety of polymers that $a = KP$ where the proportionality coefficient ($K = 17.68$) was found to be nearly independent of temperature.¹⁴ Combining this expression for the tube diameter and eqs 4–7, one easily obtains the following relationships for the number of bonds between entanglements and for the plateau modulus:

Table 2. Complex Shear Stress Moduli in Different Regimes for Different Reptation Models^a

Function	$G^*(\omega) = G'_{glass}(\omega) + G'_A(\omega) + G'_{Rouse}(\omega) + G'_{rept}(\omega) + i(G''_{glass}(\omega) + G''_A(\omega) + G''_{Rouse}(\omega) + G''_{rept}(\omega))$		
	DE ^b	MDE ^c	Milner-McLeish ^d
Storage modulus $G'(\omega)$			
Glassy regime G'_{glass} ^{e,f}	$G_\infty \left(1 - (R(\omega))^{\frac{1}{2}} \cos\left(\frac{\phi(\omega)}{2}\right)\right)$	$G_\infty \left(1 - (R(\omega))^{\frac{1}{2}} \cos\left(\frac{\phi(\omega)}{2}\right)\right)$	$G_\infty \left(1 - (R(\omega))^{\frac{1}{2}} \cos\left(\frac{\phi(\omega)}{2}\right)\right)$
Retraction regime G'_A	-	$\frac{4}{5} G_N \sum_{p=1}^{N_e} \frac{(\omega\tau_A/2p^2)^2}{1 + (\omega\tau_A/2p^2)^2}$	$G_N \int_0^{s_d} 2(1-s) \frac{(\omega\tau(s))^2}{1 + (\omega\tau(s))^2} ds$
Rouse regime G'_{Rouse}	$\frac{G_N}{n} \sum_{p=1}^{\infty} \frac{(\omega\tau_R/2p^2)^2}{1 + (\omega\tau_R/2p^2)^2}$	$\frac{G_N}{n} \sum_{p=1}^n \frac{(\omega\tau_R/p^2)^2}{1 + (\omega\tau_R/p^2)^2}$	$\frac{G_N}{n} \sum_{p=1}^N \frac{A(p)(\omega\tau_R/p^2)^2}{1 + (\omega\tau_R/p^2)^2}$
Reptating regime G'_{rept}	$G_N \sum_{p,odd}^{\infty} \frac{8}{\pi^2 p^2} \frac{(\omega\tau_d/p^2)^2}{1 + (\omega\tau_d/p^2)^2}$	$G_N \int_0^1 \frac{(\omega\tau(s))^2}{1 + (\omega\tau(s))^2} ds$	$G_N \sum_{p,odd}^{\infty} \frac{8}{\pi^2 p^2} \frac{(\omega\tau_d/p^2)^2}{1 + (\omega\tau_d/p^2)^2}$
Loss modulus $G''(\omega)$			
	DE ^b	MDE ^c	Milner-McLeish ^d
Glassy regime G''_{glass} ^{e,f}	$G_\infty (R(\omega))^{\frac{1}{2}} \sin\left(\frac{\phi(\omega)}{2}\right)$	$G_\infty (R(\omega))^{\frac{1}{2}} \sin\left(\frac{\phi(\omega)}{2}\right)$	$G_\infty (R(\omega))^{\frac{1}{2}} \sin\left(\frac{\phi(\omega)}{2}\right)$
Retraction regime G''_A	-	$\frac{4}{5} G_N \sum_{p=1}^{N_e} \frac{\omega\tau_A/2p^2}{1 + (\omega\tau_A/2p^2)^2}$	$G_N \int_0^{s_d} 2(1-s) \frac{\omega\tau(s)}{1 + (\omega\tau(s))^2} ds$
Rouse regime G''_{Rouse}	$\frac{G_N}{n} \sum_{p=1}^{\infty} \frac{\omega\tau_R/2p^2}{1 + (\omega\tau_R/2p^2)^2}$	$\frac{G_N}{n} \sum_{p=1}^n \frac{\omega\tau_R/p^2}{1 + (\omega\tau_R/p^2)^2}$	$\frac{G_N}{n} \sum_{p=1}^N \frac{A(p)\omega\tau_R/p^2}{1 + (\omega\tau_R/p^2)^2}$
Reptating regime G''_{rept}	$G_N \sum_{p,odd}^{\infty} \frac{8}{\pi^2 p^2} \frac{\omega\tau_d/p^2}{1 + (\omega\tau_d/p^2)^2}$	$G_N \int_0^1 \frac{\omega\tau(s)}{1 + (\omega\tau(s))^2} ds$	$G_N \sum_{p,odd}^{\infty} \frac{8}{\pi^2 p^2} \frac{\omega\tau_d/p^2}{1 + (\omega\tau_d/p^2)^2}$

^a All notations and crossover functions are the same as in Table 1. ^b References 7–10. ^c References 11 and 21. ^d Reference 16. ^e The same for all models, refs 21 and 24. ^f $R(\omega) = [1 + (\omega\tau_0)^2]^{-1/2}$, $\phi(\omega) = \tan^{-1}(\omega\tau_0)$.

$$N_e = \left(\frac{KM_0}{\rho}\right)^2 \left(\frac{N}{\langle R^2 \rangle}\right)^3 \quad (8)$$

$$G_N = \frac{k_B T}{K^2} \left(\frac{\rho \langle R^2 \rangle}{M_0 N}\right)^3 \quad (9)$$

where the required properties (ρ , $\langle R^2 \rangle/N$ (see below)) can be obtained from simulations of unentangled chains.

End-to-End Distance and Characteristic Ratio of the Polymer Chains. The mean-square end-to-end distance for polymer melt chains of high molecular weight can be calculated if the characteristic ratio C_∞ of the polymer is known using the relationship

$$\langle R^2 \rangle = C_\infty N b^2 \quad (10)$$

where b^2 is the mean-square bond length in the polymer backbone. C_∞ can be estimated from simulations of relatively short chains by calculating the characteristic ratio as a function of $1/N$ and then linearly extrapolating to $1/N \rightarrow 0$.¹⁸ The value of $C_\infty = 5.44$ as obtained from simulations of BD₁₁₄ is in a good agreement with experiment ($C_\infty = 5.4$).¹⁹ This C_∞ yields a molecular weight between entanglements for PBD of $M_e = 1634$ Da ($N_e = 126$) close to the reported experimental value of 1543 Da.¹⁴

IV. High-Frequency Regime (Glass Transition)

The complex shear modulus $G^*(\omega)$ is defined as a Fourier transform of the time-dependent shear stress modulus $G(t)$:⁷

$$G^*(\omega) = i\omega \int_0^\infty e^{-i\omega t} G(t) dt = G'(\omega) + iG''(\omega) \quad (11)$$

The Rouse/reptation models do not account for the elastic reaction of the melt at high frequency. At high frequencies ($\omega \gg 1/\tau_R$), it is observed experimentally that the loss modulus $G''(\omega)$ manifests a maximum that cannot be described by the reptation or Rouse approach.^{20–23} Many models have been derived for calculations of this (the glass relaxation) process.^{20–24} We found the Davidson–Cole approach²⁴ to be the most appropriate for the current treatment because it can be utilized in a form that requires no adjustable parameters when the characteristic time τ_0 for this regime is taken to be²¹

$$\tau_0 = \frac{b_{\text{dyn}} \zeta_{\text{dyn}}}{\pi^2 k_B T} = 3 \frac{C_\infty^2}{N^2} \tau_R \quad (12)$$

and the Davidson–Cole stretching exponent is taken as $1/2$. Importantly, the adequacy of this model was demonstrated for several polymers including PBD.²¹ We have taken the dynamical segment size for local motions b_{dyn} to be the static statistical segment length for PBD of 8.05 Å. The loss modulus $G''_{\text{glass}}(\omega)$ given in Table 2 exhibits a maximum at frequency $\omega_M = \sqrt{3}/\tau_0$.

To estimate the magnitude of the glassy modulus G_∞ from properties determined from simulations, we have applied an extension to the Rouse theory that takes into account high-frequency response, introduced by Marvin.^{20,25} One of the remarkable results of the theory is that it attributes the location of the maximum of $G''(\omega)$ on frequency axis to the value of G_∞ by the following relationship

$$\sqrt{3}\omega_M \zeta = \frac{24G_\infty^2 (M_0/\rho)^2}{b^2 k_B T} \quad (13)$$

This expression yields a quite simple expression for G_∞ after term rearrangement and substituting eqs 12 and 4:

$$G_\infty = \frac{\pi}{\sqrt{8}} \frac{\rho k_B T}{M_0} = \frac{\pi}{\sqrt{8}} N_e G_N \quad (14)$$

V. Results and Discussion

The original DE,^{7–10} modified DE,^{11,21} and Milner–McLeish¹⁶ reptation theories utilize the same set of input parameters obtained from MD simulations. In Figure 1 we show the time-dependent shear modulus $G(t)$ for BD₉₁₄₀ (130 000 Da) at 298 K. Predictions were obtained using the properties obtained from simulations of the BD₁₁₄ melts, specifically the Rouse time, chain dimensions, and density of the bulk polymer. As MD simulations were performed at 293, 323, and 353 K, the required parameters for 298 K were obtained by interpolating corresponding values versus temperature. As one can see, the models yield similar results for $G(t)$, with the variance becoming larger in the long-time regime where time approaches the disentanglement time τ_d . It can be seen that the time-dependent shear stress modulus calculated utilizing the modified DE and Milner–McLeish approaches relaxes faster than $G(t)$ obtained by applying the original DE method. This difference is in agreement with Doi's considerations of tube length fluctuations.^{7,11} Tube (or contour) length fluctuations of a polymer chains have a significant effect on polymer dynamics by reducing τ_d . An "effective" scaling of the longest relaxation time with respect to chain length is shown in Table 1 for all three models. Although the contour length fluctuations become negligible for very high molecular weights, their effect is not negligible for usual values of N (the order of 10 000 for common commercial polymers). In the case of BD₉₁₄₀ ($n \approx 70$), the ratio between τ_d calculated from the MDE and DE models is about 0.77, while the same ratio for the Milner–McLeish and DE models is 0.74. At short times $t \approx \tau_0$ contributions from $G_{\text{Rouse}}(t)$ are essentially the same for all models and yield a slope of $-1/2$ in accord with the theory.⁷ As one can see, this Rouse behavior is perturbed by the glass relaxation contribution $G_{\text{glass}}(t)$, which starts to dominate at times smaller than τ_0 .

We also calculated the components of the complex frequency-dependent shear stress modulus $G^*(\omega)$ for BD₉₁₄₀ at 298 K, which is shown in Figure 2. Here we compare our predictions to the experimental data of Colby et al.²⁶ on reasonably monodispersed PBD chains ($M_w/M_n < 1.1$) of the same molecular weight and with the microstructure of 35.5%/54.5%/10% 1,4-cis/1,4-trans/1,2-vinyl monomers. As can be seen, simulations of the unentangled melt yield the structural, thermodynamic, and dynamic properties required by the reptation model to yield good agreement with experiment for the linear viscoelastic properties of the higher molecular weight polymer.

The log–log plot of the real and imaginary components of $G^*(\omega)$ can be clearly divided onto three zones: the terminal or flow zone from zero frequency to $\omega = 1/\tau_d$ (10^{-11} ps⁻¹), the transition or plateau zone covering frequencies between the terminal peak and the minimum in the loss modulus $G''(\omega)$, and high frequency or glass transition zone starting at $\omega = 1/\tau_A$ (10^{-6} ps⁻¹). In the terminal zone where disentanglement occurs, $G'(\omega)$ and $G''(\omega)$ are proportional to ω^2 and ω , respectively. All models yield the right slope in this regime as shown in Figure 2, but the MDE model shows faster relaxation (occurring at higher frequencies) than the DE or Milner–McLeish models; the latter models are in better agreement with experimental data. In the transi-

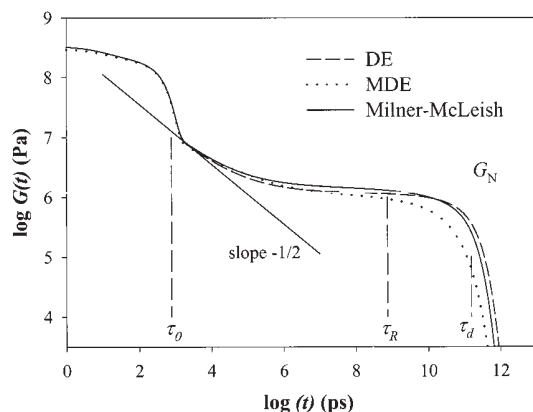


Figure 1. Time-dependent shear modulus of polybutadiene (130 000 Da) at 298 K calculated using the equations given in Table 1 for three reptation models with the $N = 9140$, $N_e = 126$, $\tau_R = 7.37 \times 10^8$ ps, $G_N = 1.41$ MPa, and $G_\infty = 0.204$ GPa.

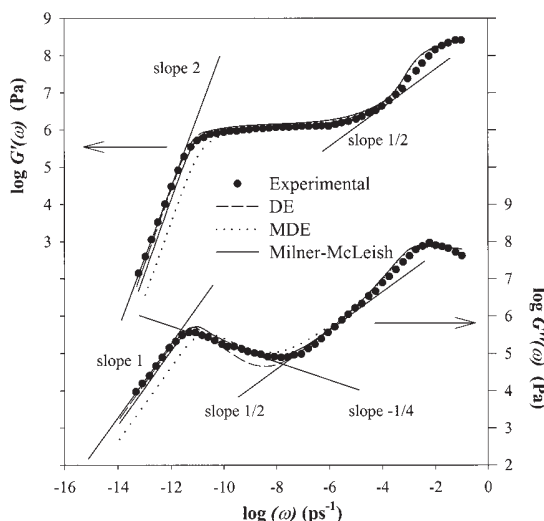


Figure 2. Computed complex frequency-dependent shear modulus of polybutadiene (130 000 Da) at 298 K compared to data of ref 26. The same parameters as in Figure 1 were used. (Straight lines are denoting slopes.)

tion zone the reptation contribution to the storage modulus $G'_{\text{rept}}(\omega)$ leads to the plateau in $G'(\omega)$, which is similar for all three models applied. The main difference between the models is manifested in the loss modulus $G''(\omega)$ plot in this frequency region. The Rouse contribution $G''_{\text{Rouse}}(\omega)$ leads to a $\omega^{-1/2}$ scaling of $G''(\omega)$ as shown for the original DE model. But the slope of $-1/2$ is much steeper than experimental data with the slope about $-1/4$, as shown in Figure 2. Such deviation from Rouse behavior was found not only for PBD but also for a number of other polymers.^{16,20–22} Agreement with experiment is improved for the models that account for contour length fluctuations. The fast-relaxing contour-length fluctuations or retraction part of $G''(\omega)$, contributing in this intermediate frequency range, gives rise to $\omega^{-1/4}$ scaling for the both MDE and Milner–McLeish models.¹⁶ Figure 2 reveals that the Milner–McLeish approach gives a better representation of the $G''(\omega)$ in the transition zone than the MDE model.

As was mentioned before, we have applied the same Davidson–Cole expressions for $G_{\text{glass}}(t)$ and $G_{\text{glass}}^*(\omega)$ for all models (Tables 1 and 2) in order to describe the behavior of the polymer at short times or in the high-frequency range. Thus, differences between models

vanish as frequency approaches $1/\tau_0$. The glass transition strongly influences dynamic mechanical behavior for frequencies greater than 10^{-4} ps $^{-1}$. The high-frequency response of PBD is not well represented by the Rouse model, as shown in Figure 2. The Davidson–Cole term of $G^*(\omega)$ gives rise to proper scaling of the storage and loss moduli.

VI. Conclusions

The main goal of the present work is to show that it is possible to predict the linear viscoelastic behavior of an entangled polymer melt utilizing properties obtained entirely from MD simulations, which to the best knowledge of the authors has never been attempted. We have demonstrated a new methodology for extrapolation of properties of short unentangled polymer chains to the highly entangled regime based on extant theoretical reptation models and semiempirical relations. We have also demonstrated that MD simulations can be used for testing of models of polymer viscoelasticity by providing physically meaningful and accurate quantities needed for the parametrization of these models.

The combination of simulation and theory allows for the accurate prediction of dynamic properties of polymer melts on time and length scales many orders of magnitude longer than are directly accessible to MD simulations. The quality of agreement obtained between simulation/theory and experiment is a consequence not only of the accurate prediction of structural, thermodynamic, and dynamic properties of the unentangled melt resulting from use of a validated, quantum chemistry based potential function but also of the validity of the viscoelastic models employed. As there is nothing specific in this approach to PBD, MD simulations of similar quality for unentangled melts of other polymers can be expected to yield accurate viscoelastic properties. Improvement in predicted properties at high frequency/short time should be possible by direct calculation of the modulus in this regime from simulation, eliminating the need for the approximate relationships for the glass relaxation utilized here. Time–temperature superposition should allow us to extend prediction of linear viscoelastic properties from simulations to much lower temperatures where time scales for the glass relaxation behavior and monomer friction coefficient (chain diffusion) are too long for direct determination from simulation.

In the nearest future we will present a continuation of this work where the methodology of direct calculations of high-frequency (glassy) modulus using the Green–Kubo method will be discussed.

Acknowledgment. This research is funded in part by the University of Utah Center for the Simulation of Accidental Fires and Explosions (C-SAFE), funded by the Department of Energy, Lawrence Livermore National Laboratory, under Subcontract B341493.

References and Notes

- (1) Smith, G. D.; Borodin, O.; Pekny, M.; Annis, B.; Londono, D.; Jaffe, R. L. *Spectrochim. Acta, Part A* **1997**, *53*, 1273.
- (2) Smith, G. D.; Yoon, D. Y.; Zhu, W.; Ediger, M. D. *Macromolecules* **1994**, *27*, 5563.
- (3) Smith, G. D.; Paul, W.; Yoon, D. Y.; Zirkel, A.; Hendricks, J.; Richter, D.; Schöber, H. *J. Chem. Phys.* **1997**, *107*, 4751.
- (4) Paul, W.; Smith, G. D.; Yoon, D. Y.; Farago, B.; Rathgeber, S.; Zirkel, A.; Willner, L.; Richter, D. *Phys. Rev. Lett.* **1998**, *80*, 2346.

- (5) Smith, G. D.; Paul, W.; Monkenbusch, M.; Willner, L.; Richter, D.; Qiu, X. H.; Ediger, M. D. *Macromolecules* **1999**, *32*, 8857.
- (6) Rouse, P. E. *J. Chem. Phys.* **1953**, *21*, 1272.
- (7) Doi, M.; Edwards, S. F. *The Theory of Polymer Dynamics*; Clarendon Press: Oxford, 1989.
- (8) Doi, M.; Edwards, S. F. *J. Chem. Soc., Faraday Trans. 2* **1978**, *74*, 818.
- (9) Doi, M.; Edwards, S. F. *J. Chem. Soc., Faraday Trans. 2* **1978**, *74*, 1789.
- (10) Doi, M.; Edwards, S. F. *J. Chem. Soc., Faraday Trans.* **1978**, *74*, 1802.
- (11) Doi, M. *J. Polym. Sci., Polym. Lett.* **1981**, *19*, 265.
- (12) de Gennes, P. G. *J. Chem. Phys.* **1971**, *55*, 572.
- (13) Smith, G. D.; Paul, W. *J. Chem. Phys.* **1998**, *102*, 1200.
- (14) Fetters, L. J.; Lohse, D. J.; Ritcher, D.; Witten, T. A.; Zirkel, A. *Macromolecules* **1994**, *27*, 4639.
- (15) Smith, G. D.; Paul, W.; Monkenbusch, M.; Richter, D., submitted to *Phys. Rev. Lett.*
- (16) Milner, S. T.; McLeish, T. C. B. *Phys. Rev. Lett.* **1998**, *81*, 725.
- (17) Graessley, W. W. *J. Polym. Sci.* **1980**, *18*, 27.
- (18) Han, J.; Jaffe, R. L.; Yoon, D. Y. *Macromolecules* **1997**, *30*, 7245.
- (19) Graessley, W. W.; Edwards, S. F. *Polymer* **1981**, *22*, 1329.
- (20) Ferry, J. D. *Viscoelastic Properties of Polymers*; John Wiley and Sons: New York, 1980.
- (21) Benallal, A.; Marin, G.; Montfort, J. P.; Derail, D. *Macromolecules* **1993**, *26*, 7229.
- (22) Glöckle, W. G.; Nonnenmacher, T. F. *Macromolecules* **1991**, *24*, 6426.
- (23) Palade, L.-I.; Verney, V.; Attané, P. *Rheol. Acta* **1996**, *35*, 265.
- (24) Davidson, D. W.; Cole, R. H. *J. Chem. Phys.* **1951**, *19*, 1484.
- (25) Marvin, R. S. In Bergen, J. T., Ed.; *Viscoelasticity: Phenomenological Aspects*; Academic Press: New York, 1960.
- (26) Colby, R. H.; Fetters, L. J.; Graessley, W. W. *Macromolecules* **1987**, *20*, 2226.

MA000439B